High Enthalpy Differential Equation-Based Estimates for Spherical/Cylindrical Forebody Shock Stand-off Distance

Lawrence DeChant[1], Ross Wagnild[2], Kyle Lynch[3], Sean Kearney[4], Justin Wagner[5]

Sandia National Laboratories, Albuquerque, NM, 87185-0825

[Abstract] Here we consider the shock stand-off distance for blunt forebodies using a simplified differential-based approach with extensions for high enthalpy dissociative chemistry effects. Following Rasmussen [4], self-similar differential equations valid for spherical and cylindrical geometries that are modified to focus on the shock curvature induced vorticity in the immediate region of the shock are solved to provide a calorically perfect estimate for shock standoff distance that yields good agreement with classical theory. While useful as a limiting case, strong shock (high enthalpy) calorically perfect results required modification to include the effects of dissociative thermo-chemistry. Using a dissociative ideal gas model for dissociative equilibrium behavior combined with shock Hugoniot constraints we solve to provide thermodynamic modifications to the shock density jump thereby sensitizing the simpler result for high enthalpy effects. The resulting estimates are then compared to high enthalpy stand-off data from literature, recent dedicated high speed shock tunnel measurements and multi-temperature partitioned implementation CFD data sets. Generally, the theoretical results derived here compared well with these data sources, suggesting that the current formulation provides an approximate but useful estimate for shock stand-off distance.

Nomenclature

D	=	local constant
F	=	local function
G	=	self-similar function
M	=	Mach number
R	=	body radius
U	=	Pre-shock velocity
α	=	dissociation fraction, local constant
δ, Δ	=	standoff distance
ε	=	shock density parameter
γ	=	ratio specific heats
ρ	=	density

Subscript

b	=	body
cyl	=	cylinder
D	=	dimensional or dissociative
e	=	equilibrium
eff	=	effective
s	=	shock
sph	=	sphere
1	=	pre-shock
2	=	post-shock
∞	=	free-stream

[1,2,3,4,5] Technical Staff, Aerosciences Dept., P.O. Box 5800, MS 0825, Albuquerque, NM, 87185, Member AIAA

American Institute of Aeronautics and Astronautics

I. Introduction

Estimation of shock stand-off distance for blunt forebodies is a fundamental problem for high enthalpy flow with direct application to reentry body physical phenomena. As a classical problem, the literature for this problem is very extensive and is perhaps best discussed by reference to several recent papers (which are important in their own right) such as Shen and Wen [1] and Sinclair and Cui [2]. Shen and Wen provide an excellent schematic representation of the physical problem which is repeated in figure 1. The earlier paper by Wen and Hornung [3] provides essential information for this class of problem with special focus on deviation from ideal gas calorically perfect behavior. The basic inviscid fluid dynamic problem may be approached in a number of ways including integral and control volume approaches but here we utilize a differential equation formalism elegantly described by Rasmussen [4] who examines an inviscid spherical/cylindrical formulation. A related analysis is developed by Hida [5].
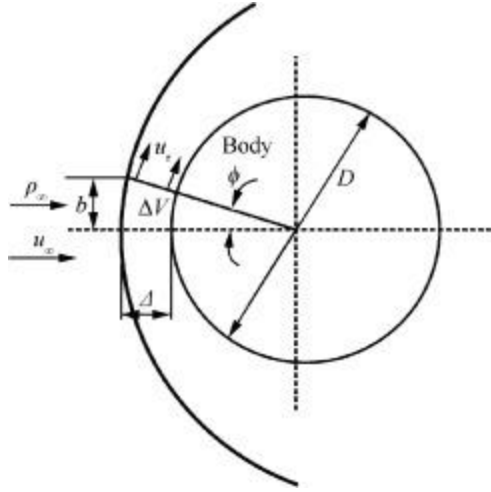

Figure 1. Schematic for shock stand-off distance problem following [1].

The structure of the paper follows with preliminary focus on solution of the self-similar differential equations describing flow of spherical and cylindrical bodies for calorically perfect problems as described by Rasmussen. Unfortunately, the Rasmussen formulation yields solutions that are in somewhat poor agreement with known stand off distance values. However, relatively simple modifications to the expressions with focus on the shock curvature induced vorticity in the immediate region of the shock offers a much-improved stand-off result. Thermodynamic behavior is included through a shock jump density parameter.

While a strong shock (high enthalpy) calorically perfect result is possible, it is of rather less utility since high enthalpy thermo-chemistry will modify the behavior of the flow. Although equilibrium and certainly non-equilibrium are perhaps best studied using experimental measurement and computational tools, the importance of this problem spurred the development of simpler analytical tools broadly described by a so-called dissociative ideal gas model Lighthill [6] and Freeman [7]. Wang et. al. [8] derive approximate but effective expressions for dissociative equilibrium behavior combined with shock Hugoniot constraints that we approximately solve to provide thermodynamic modifications to the previously employed calorically perfect shock density jump. Using an averaging procedure, we compute a best estimate for an effective specific heat ratio $\gamma \rightarrow \gamma_{eff}$ which offers an approximate but simple way to sensitize the calorically perfect model for high enthalpy dissociative effects. The resulting estimates are then compared to high enthalpy (equivalently high speed) data from literature and more recent dedicated high speed shock tunnel measurement sources. Additional comparisons are made to CFD simulations using a multi-temperature partitioned implementation in SPARC (Sandia Parallel Aerodynamics Reentry Code). Generally, the theoretical results derived here that utilize the effective specific heat ratio compared well with these data sources, suggesting that the current formulation provides an approximate but useful estimate for shock stand-off distance. Moreover, the effective specific heat ratio treatment also offers a way to sensitize other simple calorically perfect models for high enthalpy behavior.

II.   Governing Equations

Following the development of Rasmussen [4] for shocks with an appropriate separable self-similar formulation we examine spherical and cylindrical coordinate stream function-based expressions.

Spherical Shock

The spherical governing equation can be written:

$$\frac{d^2 G}{dr^2} - \frac{2}{r^2} G = \frac{(1-\varepsilon)^2}{\varepsilon^2} r^2 \tag{1}$$

Where we define the stream function: $\psi = \sin^2 \theta G(r)$ with the dimensionless variables: $G_D = \rho_\infty U_\infty^2 R_s^2 G$ and $r_D = R_s r$.   The parameter ε is defined by: $\varepsilon = \dfrac{\rho_\infty}{\rho_s}$ with $\varepsilon = \dfrac{1}{6}$ for $M \gg 1$, $\gamma = \dfrac{7}{5}$ (a common closure expression).   Explicit Mach number effects are evident via the density ratio formalism: $\varepsilon = \dfrac{(\gamma-1)M_\infty^2 + 2}{(\gamma+1)M_\infty^2}$

Equation (1) can be solved using the boundary conditions at the shock: $\left.\dfrac{dG}{dr}\right|_{r=1} = \varepsilon^{-1}$ $\quad G(1) = \dfrac{1}{2}$.   The result is:

$$G(r) = \frac{(4\varepsilon - 1)}{6\varepsilon^2} r^2 + \frac{6\varepsilon^2 - 7\varepsilon + 1}{15\varepsilon^2} r^{-1} + \frac{(\varepsilon-1)^2}{10\varepsilon^2} r^4 \tag{2}$$

Employing the condition that $G(R_b) = 0$ we have an expression that provides a relationship for R_b which is the radial location of the body.   This in turn yields a shock standoff distance as:

$$\frac{\delta_D}{R_s} = \delta = 1 - R_b \tag{3}$$

The polynomial result via equation (2) is quintic: $\dfrac{(\varepsilon-1)^2}{10\varepsilon^2} R_b^5 + \dfrac{(4\varepsilon-1)}{6\varepsilon^2} R_b^3 + \dfrac{6\varepsilon^2 - 7\varepsilon + 1}{15\varepsilon^2} = 0$ so is not solvable in closed form.   However, for $\varepsilon = \dfrac{1}{6}$ we can write the result: $R_b = 2\dfrac{\sqrt{5}}{5}$ whereby we can write:

$\delta = 1 - R_b = 1 - 2\dfrac{\sqrt{5}}{5} \approx 0.106$.   A more familiar result is the shock stand-off distances scaled by body radius as:

$\dfrac{\delta_D}{R_{bD}} = R_b^{-1} - 1 = \dfrac{\sqrt{5}}{2} - 1 \approx 0.118$

We can get a sense of the efficacy of this result by placing it in more traditional variables which are written using the nose diameter D and scaled by the density ratio: $\dfrac{\rho_\infty}{\rho_s} = \varepsilon$ so as to write:

$$\tilde{\Delta}_{sph} \equiv \frac{\Delta_{sph}}{D}\varepsilon^{-1} = \frac{R_{sD} - R_{bD}}{2R_{bD}}\varepsilon^{-1} \tag{4}$$

Using the preceding results for $\varepsilon = 1/6$ we write: $\tilde{\Delta}_{sph} = \frac{\varepsilon^{-1}}{2}\left(R_b^{-1} - 1\right) = \frac{6}{2}(\frac{\sqrt{5}}{2} - 1) \approx 0.35$. However, the classical result estimated by measurement is larger than this value and is generally accepted as $\tilde{\Delta}_{classic\_meas} = 0.41$, implying that the current result significantly underpredicts the standoff distance.

The source of this discrepancy is associated with the source term of equation (1) which in turn represents the vorticity due to the curved shock, i.e. $\frac{(1-\varepsilon)^2}{\varepsilon^2}r^2$. This result was derived to be exact at the shock location and is parameterized to be valid further into the shock. However, we propose that the vortical behavior is dominated by the value immediately behind the shock so that a simpler approximate result follows with: $r_D \approx R_D \rightarrow r = 1$ so that $\frac{(1-\varepsilon)^2}{\varepsilon^2}r^2 \rightarrow \frac{(1-\varepsilon)^2}{\varepsilon^2}$. The resulting differential equation is: $\frac{d^2G}{dr^2} - \frac{2}{r^2}G = \frac{(1-\varepsilon)^2}{\varepsilon^2}$ (with same boundary conditions gives):

$$G(r) = \frac{(2+\varepsilon)}{6\varepsilon^2}r^2 + \frac{3\varepsilon^2 - 4\varepsilon + 1}{9\varepsilon^2}r^{-1} + \frac{(1-\varepsilon)}{9\varepsilon^2}(3\ln r - 1)r^2 \tag{5}$$

We again compute R_b by solving $F(R_b, \varepsilon) \equiv \frac{(2+\varepsilon)}{6\varepsilon}R_b^3 + \frac{3\varepsilon^2 - 4\varepsilon + 1}{9\varepsilon^2} + \frac{(1-\varepsilon)}{9\varepsilon^2}(3\ln R_b - 1)R_b^3 = 0$ which for $\varepsilon = 1/6$ gives: $R_b = 0.87977$ so that $\tilde{\Delta}_{sph} = \frac{\varepsilon^{-1}}{2}\left(R_b^{-1} - 1\right) = \frac{6}{2}(0.87977^{-1} - 1) \approx 0.4100$ which is in excellent agreement with the traditional result.

The efficacy of this result suggests that an approximate explicit result for R_b would be of value. By expanding $F(R_b, \varepsilon)$ for both R_b and ε, solving for $F(R_b, \varepsilon) = 0$ we can obtain the (very) simple result: $R_b \approx 0.9832 - 0.6205\varepsilon$ so that we can write: $\tilde{\Delta}_{sph} = \frac{\varepsilon^{-1}}{2}\left(\frac{1}{0.9832 - 0.6205\varepsilon} - 1\right)$. This result is in good agreement for a range of ε values and can be recommended as a useful approximate result for the scaled spherical shock stand-off distance.

Additional modeling is possible for equation (5) as well. For example, if we replace the variable coefficient term $\frac{2}{r^2}G$ such that it takes on its maximum value as: $\frac{2}{r^2}G \rightarrow \frac{2}{R_b^2}G$ so that we solve: $\frac{d^2G}{dr^2} - \frac{2}{R_b^2}G = \frac{(1-\varepsilon)^2}{\varepsilon^2}$

$$\frac{d^2G}{dr^2} - \frac{2}{r^2}G = \frac{(1-\varepsilon)^2}{\varepsilon^2}r^2 \tag{6}$$

The resulting solution is in terms of exponential values:

$$G(r) = C_1 \exp(\sqrt{2}\,\frac{r}{R_b}) + C_2 \exp(\sqrt{2}\,\frac{r}{R_b}) + \frac{(1-\varepsilon)}{2\varepsilon^2} R_b^2 \tag{7}$$

In a completely analogous manner, we can use the same boundary conditions and solve $G(r = R_b) = 0$ to estimate:

$R_b = 0.8793$ such that: $\tilde{\Delta}_{sph} = \frac{\varepsilon^{-1}}{2}\left(R_b^{-1} - 1\right) = \frac{6}{2}(0.8793^{-1} - 1) \approx 0.412$ implying good agreement with the

empirical result. We remark, that the current approach provides little benefit over the exact solution procedure (which is relatively simple), but will be useful when determining approximations for the cylindrical problem, subsequently.

Cylindrical Shock

The cylindrical problem is formulated in a similar manner as:

$$\frac{d^2 G}{dr^2} + \frac{1}{r}\frac{dG}{dr} - \frac{1}{r^2}G = \frac{(1-\varepsilon)^2}{\varepsilon^2}G \tag{8}$$

This expression is solvable in terms of modified Bessel functions. The result is complex and not particularly informative and is therefore not expressed here. Nonetheless the associated process is precisely the same as before where $G(R_b, \varepsilon) = 0$ and can be solved numerically with $\varepsilon = 1/6$ to give: $R_b = 0.7933$ so that

$\frac{\delta_D}{R_b} = \frac{R_{sD} - R_{bD}}{R_{bD}} = \frac{1 - R_b}{R_b} = \frac{1 - 0.7933}{0.7933} \approx 0.2605$.

It is helpful at this point to examine the efficacy of this result. Convenient classical results follow from Lobb (1962) who provides the empirical result: $\delta_{cyl} = 2(0.5956)\varepsilon \approx 2(0.5956)\frac{1}{6} = 0.1985$. Wen and Hornung

(1995) use a simplified mass balance argument to show that $\delta_{cyl} = 2(\frac{1}{2})\varepsilon \approx \frac{1}{6} = 0.167$, though we emphasize

that their focus was less on the numerical value as opposed to the mass balance procedure. A method that is similar to the differential equation-based result by Hida [5] offers the limiting value i.e. $\delta_{cyl} = 2(0.1241) = 0.2482$; $M_\infty \to \infty$.

As was the case for the spherical (axi-symmetric) shock front problem, the cylindrical (planar) can be both simplified (setting r=1) and the magnitude scaling of the vorticity at the curved shock $\frac{(1-\varepsilon)^2}{\varepsilon^2}$ can be modified.

We propose that the current magnitude is too large especially at the limiting value i.e. $\frac{(1-\varepsilon)^2}{\varepsilon^2} \to \varepsilon^{-2}$ $\varepsilon \ll 1$.

The other limit is represented as: $\frac{(1-\varepsilon)^2}{\varepsilon^2} \to 0$ $\varepsilon = 1$. Thus, a regularization of this term would simply be the

arithmetic average of these two limits to give: $\frac{(1-\varepsilon)^2}{\varepsilon^2} \approx \frac{1}{2}(\varepsilon^{-2} + 0) \approx \frac{(1-\varepsilon)^2}{2\varepsilon^2}$. The associated differential equation takes the form:

$$\frac{d^2G}{dr^2} + \frac{dG}{dr} - (1 + \frac{(1-\varepsilon)^2}{2\varepsilon^2})G = 0 \tag{9}$$

The resulting expression can be solved to give:

$$G = c_1 \exp(\frac{-\varepsilon + \alpha}{2\varepsilon}r) + c_2 \exp(-\frac{-\varepsilon + \alpha}{2\varepsilon}r) \quad ; \quad \alpha = \sqrt{7\varepsilon^2 - 4\varepsilon + 2} \tag{10}$$

Using the boundary conditions $\left.\frac{dG}{dr}\right|_{r=1} = \varepsilon^{-1}$ $G(1) = 1$ we can solve $G(R_b, \varepsilon) = 0$ explicitly to give:

$$R_b = \frac{\alpha - \ln\left(\frac{2+\varepsilon+\alpha}{2+\varepsilon-\alpha}\right)\varepsilon}{\alpha} \tag{11}$$

Equation (11) gives: $R_b = 0.8252$ with $\varepsilon = 1/6$ such that $\Delta_{cyl} = \frac{1-R_b}{R_b} = \frac{1-0.8252}{0.8252} \approx 0.2112$ which better spans the empirical solution described previously. Equation (11) in turn can be expanded for small ε to give the convenient expression for δ_{cyl} as:

$$\delta_{cyl} = \Delta_{cyl} = (1.236 - 0.0418\varepsilon + 1.453\varepsilon^2)\varepsilon \quad ; \quad 1/6 < \varepsilon < 1/2 \tag{12}$$

There is value in examining the density ratio scale version of this result i.e. $\tilde{\Delta}_{cyl} = \varepsilon^{-1}\frac{\delta_{cylD}}{2R} = \frac{\varepsilon^{-1}}{2}\delta_{cyl}$ which for

$\varepsilon = 1/6$ yields: $\tilde{\Delta}_{cyl} = \varepsilon^{-1}\frac{\delta_{cylD}}{2R} = \frac{6}{2}\delta_{cyl} = 0.66$ larger as compared the classical spherical result

$\tilde{\Delta}_{sph} = \frac{\varepsilon^{-1}}{2}\delta_{sph} \approx 0.4100$. For reference we write the two expressions:

$$\tilde{\Delta}_{cyl} = \frac{\varepsilon^{-1}}{2}\delta_{cyl} = \frac{1}{2}(1.236 - 0.0418\varepsilon + 1.453\varepsilon^2) \quad ; \quad 1/6 < \varepsilon < 1/2 \tag{13}$$

and

$$\tilde{\Delta}_{sph} = \frac{\varepsilon^{-1}}{2}\delta_{sph} = \frac{\varepsilon^{-1}}{2}\left(\frac{1}{0.9832 - 0.6205\varepsilon} - 1\right) \quad ; \quad 1/6 < \varepsilon < 1 \tag{14}$$
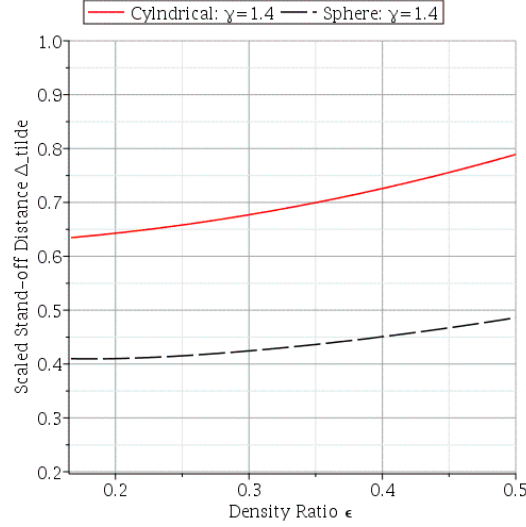
Figure 1. Scaled shock standoff distance $\tilde{\Delta} = \dfrac{\varepsilon^{-1}}{2}\delta$ for spherical and cylindrical problems as a function of density

ratio $\varepsilon = \dfrac{(\gamma-1)M_\infty^2 + 2}{(\gamma+1)M_\infty^2}$ for $\gamma = 7/5$ using the simplified expressions in equations (13) and (14).

Equilibrium Chemistry Effects

The preceding models provide a useful estimate for standoff distance for non-chemically reacting flows. However, many strong shock, high-speed flow problems are characterized by chemical dissociation of the constituent gas field, which significantly modifies standoff problem behavior via the associated density field. The density ratio term $\left(\dfrac{\rho_s}{\rho_\infty}\right)$ is the term that we will sensitize for the chemically activated problem. Recall that for a non-reacting ideal

gas we have: $\dfrac{\rho_s}{\rho_\infty} = \varepsilon^{-1} = \dfrac{(\gamma+1)M_\infty^2}{(\gamma-1)M_\infty^2 + 2}$ and that for (γ=1.4) $M_\infty \gg 1 \rightarrow \dfrac{\rho_s}{\rho_\infty} = \varepsilon^{-1} = 6$. Since the density

ratio is the principal connection to the previous stand-off computations, the goal hear is to derive expressions for the density ratio that honor chemistry effects. We emphasize, that we are utilizing the so-called constant density ratio approximation, whereby the post-shock density ratio is utilized within the standoff layer.

An analogous result for the density ratio associated with a chemically reacting non-equilibrium/equilibrium is possible using a simplified model called an ideal dissociating gas (Lighthill, Freeman etc.). Their formulation is based upon a dissociation fraction parameter α. The α parameter describes the degree of dissociation at any state with $\alpha = 0$ implying the absence of chemical dissociation and $\alpha = 1$ complete dissociation. This parameter is in

turn governed by a rate equation: $\dfrac{d\alpha}{dx} = \dfrac{C}{L}\left(\left(\dfrac{\rho_D}{\rho}\right)\exp\left(-\left(\dfrac{T}{T_D}\right)^{-1}\right) - \dfrac{\alpha^2}{1-\alpha}\right)$, where L is an appropriate length

scale, and both a dissociation temperature T_D and dissociation density ρ_D are defined. These parameters are given for several gases with sample values for nitrogen are:
  T_D =   113200 K
  ρ_D =   1.3E5 kg/m^3
Analogous results are available for oxygen as:
  T_D =   59500 K
  ρ_D =   1.5E5 kg/m^3

We emphasize, that rate equation associated with equation (16) implies a non-equilibrium condition while for

$\dfrac{d\alpha}{dx} = 0$ the system is in equilibrium such that $\left(\dfrac{\rho_D}{\rho_e}\right)\exp(-\left(\dfrac{T_e}{T_D}\right)^{-1}) - \dfrac{\alpha_e^2}{1-\alpha_2}$.

Deferring the computation of the dissociation fraction parameter, α we can use appropriate shock-Hugoniot conservation expressions to estimate the density ratio. The (approximate) closures utilized by Wang et. al. [8] takes the form:

$$\frac{\rho}{\rho_\infty} = \varepsilon^{-1} = \frac{u_\infty}{u} = \frac{1}{2}\left(1 - \sqrt{1 - \frac{2(1+\alpha)}{\mu}\left(\frac{T}{T_D}\right)}\right)^{-1}$$

$$\frac{T}{T_D} = \frac{\mu - \alpha}{f(\varepsilon_0) + 0.55\alpha}$$

(15)

Where: $\mu = \dfrac{u_\infty^2}{2RT_D}$. The term $f(\varepsilon_0)$ is chosen such that for $\alpha \to 0$ in equation (17) that

$\varepsilon^{-1} = \dfrac{(\gamma+1)M_\infty^2}{(\gamma-1)M_\infty^2 + 2}$. The explicit solution for $f(\varepsilon_0)$ is trivial as:

$$f(\varepsilon_0) = \frac{(\gamma+1)^2 M_\infty^4}{4[(\gamma-1)M_\infty^2 + 2](M_\infty^2 - 1)}$$

(16)

We emphasize that the first expression in equation (15) follows from the Rankine-Hugoniot expression, but the 2nd is a (useful) empirical result.

Obviously, to utilize equation (15) it is necessary to be able to estimate the dissociation fraction. As indicated dissociation fraction is governed by equation (16) which balances chemical reaction versus recombination. An important limiting case is associated with equilibrium whereby $\dfrac{d\alpha}{dx} = 0$ such that

$\left(\dfrac{\rho_D}{\rho_e}\right)\exp(-\left(\dfrac{T_e}{T_D}\right)^{-1}) - \dfrac{\alpha_e^2}{1-\alpha_e}$. While one can formulate a fundamentals-based result for α_e a semi-empirical model derived by Wang is probably adequate as:

$$\alpha_e = \frac{\mu + 0.011D - 0.39}{0.0015D^2 - 0.062D + 1.8} \quad ; \quad D = \ln(\frac{\rho_d}{\rho_\infty})$$

(17)

Unfortunately, equation (17) is not valid for both $\alpha_e \ll 1$ and $\mu \ll 1$ where equation (19) yields values for $\alpha_e < 0$ which are physically invalid. To gain a sense of the correct behavior in this limit, let's examine:

$\left(\dfrac{\rho_D}{\rho_e}\right)\exp(-\left(\dfrac{T_e}{T_D}\right)^{-1}) - \dfrac{\alpha_e^2}{1-\alpha_e}$ with $\dfrac{T_e}{T_D} = \dfrac{\mu - \alpha_e}{4.45 + 0.55\alpha_e}$ by expanding both sides for $\alpha_e \ll 1$ to give:

$$1-\frac{(0.55\mu+4.45)}{\mu^2}\alpha_e = 0+..+O(\alpha_e^2)$$
(18)

Which is easily solved to give: $\alpha_e = \dfrac{20\mu^2}{11\mu+89}$. Notice that for $\alpha_e \propto \mu^2$ $\mu << 1$

and $\alpha_e \propto \dfrac{20\mu^2}{11\mu+89} \propto \mu$ $\mu >> 1$. Thus, we could modify equation (ignoring the effect of D) to write:
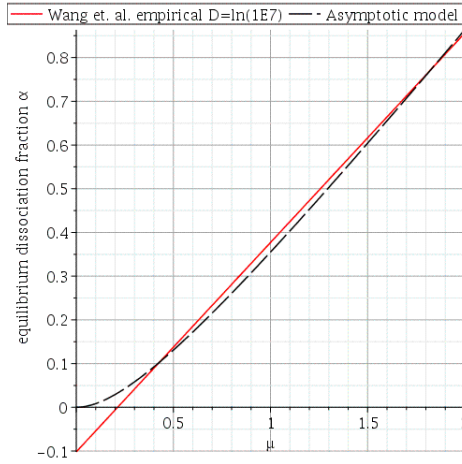
$$\alpha_e \approx \frac{\mu^2}{(0.001D+1.8)\mu+1}$$
(19)

Figure 3. Estimates for equilibrium dissociation fraction as a function of $\mu = \dfrac{u_\infty^2}{2RT_D}$ for

$D = \ln(\dfrac{\rho_d}{\rho_\infty}) = \ln(1E7)$ using equation (19) $\alpha_e \approx \dfrac{\mu^2}{(0.001D+1.8)\mu+1}$.

Using these expressions, we now have a suitable approach to modify the standoff formulation to be valid for chemically reacting equilibrium flows:

$$\varepsilon = \frac{1}{2}\left(1-\sqrt{1-\frac{2(1+\alpha)}{f(\varepsilon_0)+0.55\alpha}}\right) \quad ; \quad \alpha_e \approx \frac{\mu^2}{(0.001D+1.8)\mu+1}$$
(20)

where we emphasize that the parameters $D = \ln(\dfrac{\rho_d}{\rho_\infty})$ and $\mu = \dfrac{u_\infty^2}{2RT_D} = \dfrac{\gamma}{2}M_\infty^2\left(\dfrac{T_\infty}{T_D}\right)$ are known from the free

stream conditions since both ρ_d and T_D are known e.g. T_D=113200 K and ρ_D=1.3E5 kg/m^3. Equation (20) provides access to the density ratio as required by our previous standoff models. Let's plot the corresponding

density ratio as function of freestream Mach number for $\dfrac{T_\infty}{T_D} = \dfrac{293}{113200}$, $D \approx 11$ and compare to the ideal case:

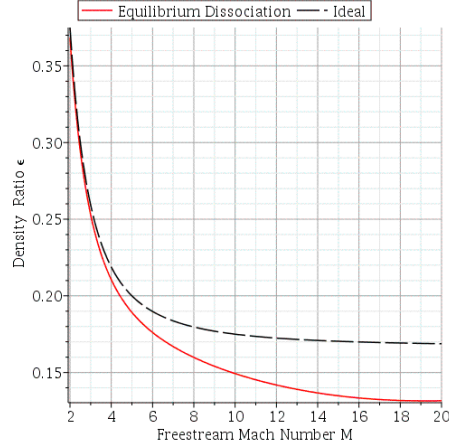$$\varepsilon_{ideal} = \frac{(\gamma - 1)M_\infty^2 + 2}{(\gamma + 1)M_\infty^2}$$

Figure 4. Density ratio ε including equilibrium dissociation compared with ideal case: $\varepsilon_{ideal} = \dfrac{(\gamma - 1)M_\infty^2 + 2}{(\gamma + 1)M_\infty^2}$

The derivation of the modified curve presented in figure 4. suggests that one may be able to estimate an effective ratio of specific heats $\gamma \rightarrow \gamma_{eff}$ for the preceding curves. Indeed, if one were to compute the integral for equation (20) as a function of Mach number between M=2 and M=20 and a demand that the effective expression honor this result, we can write:

$$\int_2^{20} \varepsilon dM_\infty = 2.92 = \int_2^{20} \frac{(\gamma_{eff} - 1)M_\infty^2 + 2}{(\gamma_{eff} + 1)M_\infty^2} dM_\infty = \frac{180\gamma_{eff} - 171}{10(\gamma_{eff} + 1)} \tag{21}$$

Equation (21) can be readily solved to give: $\gamma_{eff} = 1.33$. Let's in turn examine the associated curves as expressed using this effective value:
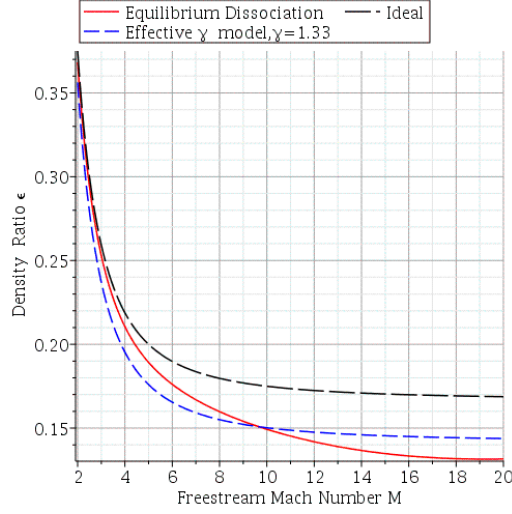
Figure 5. Density ratio ε using effective closure with $\varepsilon \approx \dfrac{(\gamma_{eff}-1)M_\infty^2+2}{(\gamma_{eff}+1)M_\infty^2}$ $\gamma_{eff}=1.33$

We note, that equation (20) uses γ as part of the definition of the dimensionless velocity ratio $\mu = \dfrac{\gamma}{2}M_\infty^2\left(\dfrac{T_\infty}{T_D}\right)$ and in equation (16) that traditionally we would use the low enthalpy result $\gamma = 7/5$ and then estimate an effective specific heat ratio γ_{eff}. Obviously, one could use the effective result in these expressions so as to obtain a more consistent result. We warn, however, that the formulation for equation (20) was implicitly based on $\gamma = 7/5$ and an iterative approach will not be effective. Nonetheless, there is value in broadly considering the trend associated with solving equation (20) where we introduce: $\gamma = \dfrac{7}{5}+\gamma'+\ldots$. We can use the same expression in $\varepsilon = \dfrac{(\gamma-1)M_\infty^2+2}{(\gamma+1)M_\infty^2}$. Integration of equation (20) is cumbersome, but we can evaluate the result (collocation) for M=10 for both expressions so as to write:

$$0.1493+0.2682\gamma' = \frac{7}{40}+\frac{11}{32}\gamma' \rightarrow \gamma = \frac{7}{5}+\gamma' \approx 1.06 \tag{22}$$

Obviously, the result of equation (22) with $\gamma \approx 1.06$ is implausibly low (high temperature air is usually bounded as $\dfrac{9}{7}\approx 1.29 < \gamma < \dfrac{5}{3}\approx 1.67$ which we attribute to the semi-empirical nature of equation (20) being formulated for $\gamma = \dfrac{7}{5}$. Nonetheless, the lower value derived in equation (22) suggests that the closure result suggested by equation (21) and depicted in figure (5) with $\gamma_{eff}=1.33$ may be slightly too large. We discuss this trend subsequently. Access to a reliable expression for the equilibrium chemistry sensitized model for the density ratio parameter ε provides a simple and direct method to determine the effect of chemistry on density field and thereby the shock stand-off distance.

III. Results

Shock Stand-Off Data Comparison

Shock standoff simulation and measurement are available to better understand the efficacy of the models developed here.   A typical problem would involve comparison for measured stand-off distance as a function of velocity or Mach number. Nonaka et al. [9] performed a suite of ballistic range standoff measurements for hemi-spherical bodies to provide direct data that demonstrate the effect of dissociative thermo-chemistry for high Mach number problems.   Considering Nonaka's measurements for the parameter $\rho_\infty R = 2.0E-4$. Under these conditions for R=15 mm we estimate the ambient temperature is approximately 350K permitting us to reduce the data sets.

For spherical standoff-behavior, we can combine the previously derived closure expressions to write:

$$\frac{\Delta_D}{R} = \frac{1}{2}\left(\frac{1}{0.9832 - 0.6205\varepsilon} - 1\right) \quad ; \quad \varepsilon \approx \frac{(\gamma_{eff} - 1)M_\infty^2 + 2}{(\gamma_{eff} + 1)M_\infty^2} \quad ; \quad \gamma_{eff} = 1.33 \tag{23}$$

Which can be directly applied to compare to the Nonaka et al. 1997 data in figure 6. As presented in the figure 6, there is reasonably good agreement between the theory summarized by equation (23) and measurement
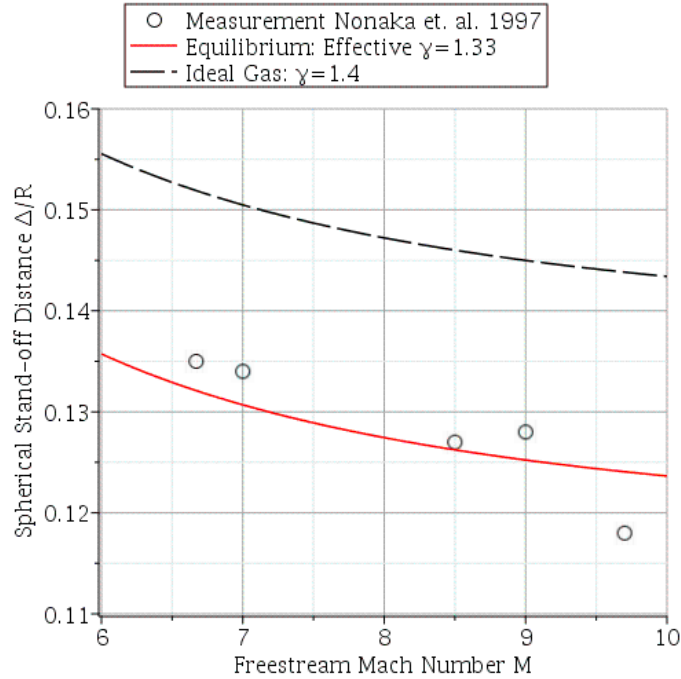

Figure 6. Comparison between measurement of Nonaka et. al. 1997 and theory as described by equation (23) for spherical standoff distance.

A related measurement is described by Lynch et. al. (2022) for a preliminary run for their hypersonic shock tunnel facility. The flow conditions are for a $T_0 = 3700K$, $M_\infty = 8-9$ (we use $M_\infty \approx 8.5$) condition with the Schlieren depicted in figure 7 demonstrating the measurement for a spherical body.
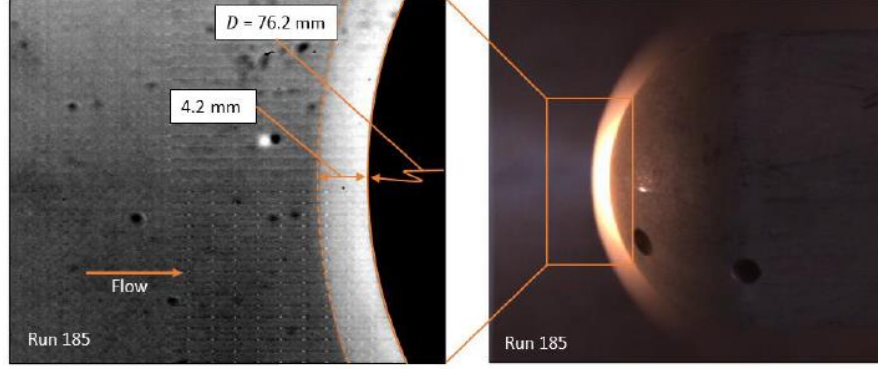

Figure 7. Schlieren depicting shock stand-off measurement for $M_\infty \approx 8.5$ for shock tunnel flow.

Using equation (23) we can readily estimate the shock standoff distance as presented in figure 8. As shown in the figure, the standoff distance is over predicted (by about 15% relative error) when using the effective closure $\gamma_{eff} = 1.33$. As discussed previously, the value $\gamma_{eff} = 1.33$ may be slightly too large due to a formulation bias. We can gain some sense of the effect of slightly smaller value for the effective specific heat ratio by consider a 5% decrease such that $\gamma_{eff} = 1.26$. As shown in figure 8. this decrease in the specific heat ratio better estimates the standoff location.
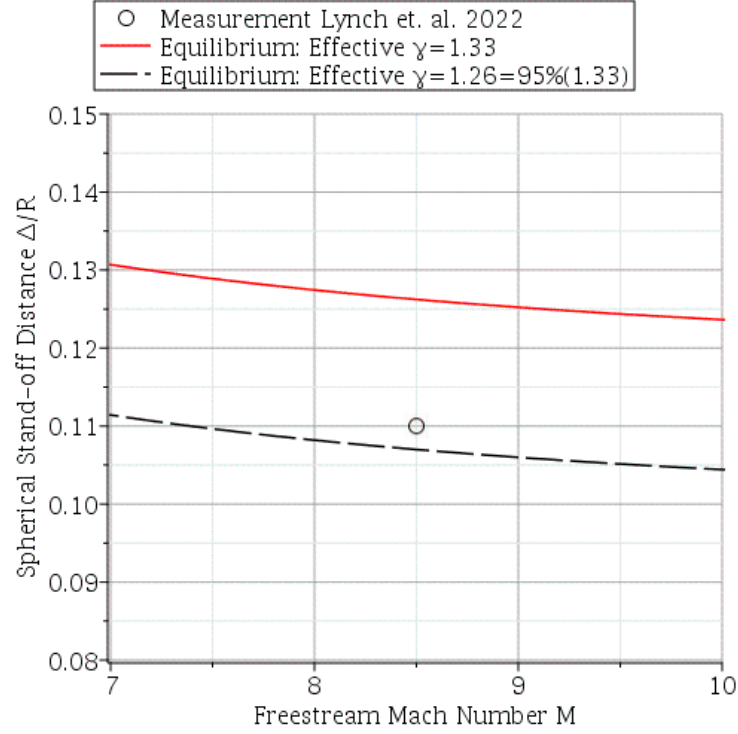
Figure 8. Comparison between measurement of Lynch et. al. (2022) and theory as described by equation (23) for spherical standoff distance.

Additional comparisons are possible using high performance computing tools such as SPARC (Sandia Parallel Aerodynamics Reentry Code) [11]. Following [11], SPARC is a compressible computational fluid dynamics (CFD) code developed to analyze aerodynamics and aerothermodynamics problems primarily for NNSA's nuclear security programs. SPARC solves the Navier–Stokes and Reynolds-Averaged Navier–Stokes (RANS turbulence models) equations on structured and unstructured grids using a cell-centered finite volume discretization scheme.

Include comparison to SPARC Multi-temp simulation here.

IV. Conclusion

In summary, we have solved a set of classical self-similar differential equations describing flow over spherical and cylindrical bodies for calorically perfect thermodynamic conditions as described by Rasmussen [3]. Limitations for the Rasmussen formulation as compared to classical stand-off results were relaxed by focusing on the shock curvature induced vorticity in the immediate region of the shock which offered a much-improved stand-off result. Thermodynamic behavior is included through a shock jump density parameter. High enthalpy thermo-chemistry modifications were introduced in the simpler model using the so-called dissociative ideal gas model Lighthill [6] and Freeman [7] with additional approximate equilibrium expressions by Wang et. al. [8] to provide thermodynamic modifications to the previously employed calorically perfect shock density jump. Using an averaging procedure, a best estimate for an effective specific heat ratio $\gamma \rightarrow \gamma_{eff}$ was derived which yielded an approximate but simple way to sensitize the calorically perfect model for high enthalpy dissociative effects. The resulting estimates were compared to high-speed data from literature and more recent dedicated high speed shock tunnel measurement

sources.   Additional comparisons were made to CFD simulations using a multi-temperature partitioned implementation in SPARC (Sandia Parallel Aerodynamics Reentry Code). Generally, the theoretical results derived here that utilize the effective specific heat ratio compared well with these data sources, suggesting that the current formulation provides an approximate but useful estimate for shock stand-off distance. Moreover, the effective specific heat ratio treatment may also a way to sensitize other simple calorically perfect models for high enthalpy behavior. Additional effort to explore the connection between the effective γ estimated here and its application to other high enthalpy flow problems may be of value.

V. Acknowledgements

VI. References

1. Shen, Hua, Wen, Chi-Yung, "Theoretical Investigation of Shock Stand-Off Distance for Non-Equilibrium Flows Over Spheres," *Chinese Journal of Aeronautics*, V. 31, 5, pp. 990-996, 2018.
2. Sinclair, J., Cui, X., "A Theoretical Approximation of the Shock Standoff Distance for Supersonic Flows Around a Circular Cone," *Physics of Fluids*, 29 026102, 2017.
3. Wen, C., Y., Hornung, H. G., "Non-equilibrium Dissociative Flow Over Spheres," V. 299 pp. 389-405 2006.
4. Rasmussen, M. L., *Hypersonic Flow*, Wiley, NY, 1994.
5. Hida, K., "An Approximate Study of the Detached Shock Wave in Front of a Circular Cylinder and a Sphere," *Journal of the Physical Society of Japan*, V. 8, pp 740-745, 1953.
6. Lighthill, M. J., "Dynamics of a Dissociating Gas, Part I, Equilibrium Flow," *Journal of Fluid Mechanics*, 2, 1, pp. 1-32, 1957.
7. Freeman, N. C., "Non-equilibrium Flow of an Ideal Dissociating Gas," *Journal of Fluid Mechanics*, V. 4, 4, pp. 407-425, 1958.
8. Wang, Z., Bao, L., Tong, B., "Theoretical Modeling of the Chemical Non-equilibrium Flow Behind a Normal Shock Wave," *AIAA Journal*, V. 50, 2 pp. 494-499, 2012.
9. Nonaka, S., Mizuno, H., Takayama, K., "Ballistic Range Measurement of Shock Shapes, in Intermediate Hypersonic Regime, AIAA Paper," AIAA-99-1025.
10. Lynch, K., Grasser, T., Farias, P., Daniel, K., Spillers, R., Downing C., Wagner, J., "Design and Characterization of the Sandia Free-Piston Reflected Shock Tunnel," AIAA paper, 2022-0968.
11. Howard, M., Bradley, A., Bova, S., Overfelt, J., Wagnild, R., Dinzl, D, Hoemmen, M., Kinvex, A., "Toward a Performance Portable Compressible CFD Code," AIAA paper 2017-4407.